

---

# Model of Imperfect Interfaces in Composite Materials and Its Numerical Solution by FETI Method

Jaroslav Kruis, Jan Zeman, and Pavel Gruber

Department of Mechanics, Faculty of Civil Engineering, Czech Technical University in Prague [jk@cml.fsv.cvut.cz](mailto:jk@cml.fsv.cvut.cz), [zeman@cml.fsv.cvut.cz](mailto:zeman@cml.fsv.cvut.cz), [gruber@fsv.cvut.cz](mailto:gruber@fsv.cvut.cz)

**Summary.** Analysis of material interfaces in composite materials is in the center of attention of many material engineers. The material interface influences significantly the overall behaviour of composite materials. While the perfect bond on material interface is modelled without larger difficulties, the imperfect bond between different components of composite materials still causes some obstacles. This contribution concentrates on application of the FETI method to description of the imperfect bond.

## 1 Introduction

The overall behavior of the engineering materials and structures is significantly affected or even dominated by the presence of interfaces, i.e. internal boundaries arising from material discontinuities. Therefore, considerable research efforts within the engineering community have been focused to adequately describe and simulate the interfacial behavior under general loading conditions. A successful approach to this problem is offered by the cohesive zone concept published in reference [3], in which the bulk material is assumed to be damage-free, whereas the interface response is described by means of inelastic damage law. The interface model itself is formulated in terms of displacement jumps and cohesive tractions bridging the interface, with the elastic stiffness as the basic constitutive parameter. Initially, the stiffness is set to a large value (modeling almost perfect bonding) that gradually decreases with increasing load. For the standard displacement-based finite element approximations, this gives a rise to numerical difficulties manifested in oscillations of interfacial tractions for stiff interfaces and non-physical penetration of adjacent bodies for imperfect bonding. The purpose of this contribution is to demonstrate that these limitations can be overcome by duality solvers based on FETI method.

## 2 Interface Model

The constitutive description adopted in this work is based on the Ortiz-Pandolfi model proposed in [7]. Detailed description of the model of the imperfect material

interface can be found in reference [2]. The model is based on three state variables, 33  
namely the domain displacement field,  $\mathbf{u}^{(j)}(\mathbf{x})$ , the interfacial displacement jump, 34  
 $[[\mathbf{u}^{(i,j)}]](\mathbf{x})$ , and the interfacial damage parameter,  $\omega^{(i,j)}(\mathbf{x})$ . The superscript ( $j$ ) 35  
denotes the subdomain number while the two superscripts ( $i, j$ ) denote the interface 36  
between the  $i$ -th and  $j$ -th subdomains. 37

The kinematics of the interface is quantified by the normal and tangential component 38  
of the displacement jump, provided by 39

$$[[u_n^{(i,j)}]](\mathbf{x}) = [[\mathbf{u}^{(i,j)}]](\mathbf{x}) \cdot \mathbf{n}^{(j)}(\mathbf{x}), \quad (1)$$

where  $\mathbf{n}^{(j)}(\mathbf{x})$  denotes the normal vector and the tangential component is in the form 40

$$[[\mathbf{u}_t^{(i,j)}]](\mathbf{x}) = [[\mathbf{u}^{(i,j)}]](\mathbf{x}) - [[u_n^{(i,j)}]](\mathbf{x})\mathbf{n}^{(j)}(\mathbf{x}). \quad (2)$$

Note that the non-penetration condition hold, i.e. the normal component must remain 41  
non-negative. Following [3], these quantities are combined into an effective opening 42

$$\delta(\mathbf{x}, [[\mathbf{u}^{(i,j)}]](\mathbf{x})) = \sqrt{[[u_n^{(i,j)}]]^2(\mathbf{x}) + \beta^2 [[\mathbf{u}_t^{(i,j)}]]^2(\mathbf{x})} \quad (3)$$

in which  $\beta$  denotes a constitutive parameter, also called the mode mixity parameter, 43  
to be determined. This gives rise to an equivalent effective traction,  $\sigma$ , see [7]. In 44  
addition, the state of an interface is quantified by an internal damage variable,  $\omega$ , 45  
with  $\omega(\mathbf{x}) = 0$  corresponding to a perfect bonding at  $\mathbf{x}$ , whereas  $\omega(\mathbf{x}) = 1$  indicates 46  
a fully damaged interface point. 47

In order to assemble the functional of energy, several energy densities are needed. 48  
The density of internal energy has the form 49

$$e_{vol}^{(j)}(\mathbf{x}, \mathbf{u}^{(j)}(\mathbf{x})) = \frac{1}{2} \left( \boldsymbol{\varepsilon}(\mathbf{u}^{(j)}(\mathbf{x})) \right)^T \mathbf{D} \boldsymbol{\varepsilon}(\mathbf{u}^{(j)}(\mathbf{x})), \quad (4)$$

where  $\boldsymbol{\varepsilon}^{(j)}(\mathbf{u}^{(j)}(\mathbf{x}))$  denotes the strain,  $\mathbf{D}$  denotes the stiffness matrix of the material. 50  
The internal energy functional can be written as 51

$$E_{vol}^{(j)}(\mathbf{u}^{(j)}(\mathbf{x})) = \int_{\Omega^{(j)}} e_{vol}^{(j)}(\mathbf{x}, \mathbf{u}^{(j)}(\mathbf{x})) d\Omega. \quad (5)$$

The potential energy of external forces has the form 52

$$E_{ext}^{(j)}(\mathbf{u}^{(j)}(\mathbf{x}), t) = - \int_{\Omega^{(j)}} \mathbf{u}^{(j)}(\mathbf{x}) \cdot \mathbf{b}(\mathbf{x}, t) d\Omega - \int_{\Gamma_t^{(j)}} \mathbf{u}^{(j)}(\mathbf{x}) \cdot \mathbf{t}(\mathbf{x}, t) d\Gamma, \quad (6)$$

where  $\mathbf{b}(\mathbf{x}, t)$  denotes the vector of volume forces,  $\mathbf{t}(\mathbf{x}, t)$  denotes the vector of surface 53  
traction and  $\Gamma_t^{(j)}$  is the part of the boundary of the  $j$ -th subdomain where the surface 54  
tractions are prescribed. The energy-based description involves the stored energy 55  
function defined as 56

$$e_{int}(\mathbf{x}, [[\mathbf{u}]](\mathbf{x}), \omega(\mathbf{x})) = \frac{1}{2} \frac{G}{\Delta^2} \frac{1 - \omega(\mathbf{x})}{\omega(\mathbf{x})} \delta^2, \quad (7)$$

where  $\Delta$  is the critical interface opening and  $G$  is the fracture toughness of an interface. This form is consistent with the linear softening law drawn in Fig. 1. Note that the stiffness associated with a partially damaged interface with the damage parameter,  $\omega$ , is obtained as a slope of the line OA. The energy dissipated by changing the internal variable from  $\omega_1$  to  $\omega_2$  is given by

$$d = \begin{cases} G(\mathbf{x})(\omega_2(\mathbf{x}) - \omega_1(\mathbf{x})) & \forall \mathbf{x} \in \Gamma_{int} : \omega_1(\mathbf{x}) \leq \omega_2(\mathbf{x}), \\ \infty & otherwise, \end{cases} \quad (8)$$

where the term  $\infty$  refers to the fact that the damage variable cannot decrease during the loading process. The interfacial dissipation distance is defined

$$D(\omega_1(\mathbf{x}), \omega_2(\mathbf{x})) = \int_{\Gamma_{int}} d(\mathbf{x}, \omega_1(\mathbf{x}), \omega_2(\mathbf{x})) d\Gamma. \quad (9)$$

The interfacial energy functional has the form

$$E_{int}(\llbracket \mathbf{u} \rrbracket(\mathbf{x}), \omega(\mathbf{x})) = \int_{\Gamma_{int}} e_{int}(\mathbf{x}, \llbracket \mathbf{u} \rrbracket(\mathbf{x}), \omega(\mathbf{x})) d\Gamma, \quad (10)$$

where  $\Gamma_{int}$  denotes the interface between subdomains.

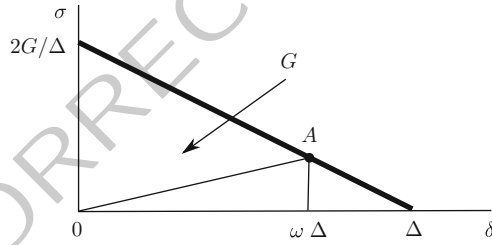


Fig. 1. Interfacial constitutive law

The description of the material interface is based on incremental solution where the state variables at the  $k$ -th step  $\mathbf{u}_{k-1}(\mathbf{x})$ ,  $\llbracket \mathbf{u} \rrbracket_{k-1}(\mathbf{x})$ ,  $\omega_{k-1}(\mathbf{x})$  are known. Then, the energy functional has the form

$$\Pi_k(\mathbf{u}(\mathbf{x}), \llbracket \mathbf{u} \rrbracket(\mathbf{x}), \omega(\mathbf{x})) = \sum_{j=1}^n E_{vol}^{(j)}(\mathbf{u}^{(j)}(\mathbf{x})) + \quad (11)$$

$$\sum_{j=1}^n E_{ext}^{(j)}(\mathbf{u}^{(j)}(\mathbf{x})) + E_{int}(\llbracket \mathbf{u} \rrbracket(\mathbf{x}), \omega(\mathbf{x})) + D(\omega_{k-1}(\mathbf{x}), \omega(\mathbf{x}))$$

and the following minimization problem is solved

$$(\mathbf{u}_k(\mathbf{x}), \llbracket \mathbf{u} \rrbracket_k(\mathbf{x}), \omega_k(\mathbf{x})) = \arg \min_{(\mathbf{u}(\mathbf{x}), \llbracket \mathbf{u} \rrbracket(\mathbf{x}), \omega(\mathbf{x}))} \Pi_k(\mathbf{u}(\mathbf{x}), \llbracket \mathbf{u} \rrbracket(\mathbf{x}), \omega(\mathbf{x})). \quad (12)$$

The discretization of displacements and strains has the form

70

$$\mathbf{u}^{(j)}(\mathbf{x}) \approx \mathbf{u}_h^{(j)}(\mathbf{x}) = \mathbf{N}_{u,h}^{(j)}(\mathbf{x}) \mathbf{u}_h^{(j)}, \quad (13)$$

$$\boldsymbol{\varepsilon}^{(j)}(\mathbf{x}) \approx \boldsymbol{\varepsilon}_h^{(j)}(\mathbf{x}) = \mathcal{B}_{u,h}^{(j)}(\mathbf{x}) \mathbf{u}_h^{(j)}, \quad (14)$$

where  $\mathbf{N}_{u,h}^{(j)}(\mathbf{x})$  denotes the matrix of basis functions and  $\mathcal{B}_{u,h}^{(j)}(\mathbf{x})$  denotes the strain-displacement matrix. The displacement jump is discretized in the form

71

72

$$\llbracket \mathbf{u}^{(i,j)} \rrbracket(\mathbf{x}) \approx \llbracket \mathbf{u}_h^{(i,j)} \rrbracket(\mathbf{x}) = \mathbf{N}_{\llbracket u \rrbracket,h}^{(i,j)}(\mathbf{x}) \llbracket \mathbf{u}^{(i,j)} \rrbracket_h \quad (15)$$

and the damage parameter can be expressed

73

$$\omega^{(i,j)}(\mathbf{x}) \approx \omega_h^{(i,j)}(\mathbf{x}) = \mathbf{N}_{\omega,h}^{(i,j)}(\mathbf{x}) \omega_h^{(i,j)}. \quad (16)$$

After discretization, the functional of energy (11) has the form

74

$$\begin{aligned} \Pi_k(\mathbf{u}_h, \llbracket \mathbf{u} \rrbracket_h, \omega_h) &= \frac{1}{2} \sum_{j=1}^n \mathbf{u}_h^{(j)T} \mathbf{K}^{(j)} \mathbf{u}_h^{(j)} - \sum_{j=1}^n \mathbf{u}_h^{(j)T} \mathbf{f}_h^{(j)} + \\ &+ \frac{1}{2} \llbracket \mathbf{u} \rrbracket_h^T \mathbf{K}_{int}(\omega_h) \llbracket \mathbf{u} \rrbracket_h + \omega_h^T \mathbf{p}_h, \end{aligned} \quad (17)$$

where the stiffness matrix has the classical form

75

$$\mathbf{K}^{(j)} = \int_{\Omega^{(j)}} \mathcal{B}_{u,h}^{(j)T} \mathbf{D} \mathcal{B}_{u,h}^{(j)} d\Omega \quad (18)$$

and the vector of prescribed forces is defined as

76

$$\mathbf{f}_h^{(j)} = \int_{\Omega^{(j)}} \mathbf{N}_{u,h}^{(j)T}(\mathbf{x}) \mathbf{b}(\mathbf{x}) d\Omega + \int_{\Gamma_t^{(j)}} \mathbf{N}_{u,h}^{(j)T}(\mathbf{x}) \mathbf{t}(\mathbf{x}, t) d\Gamma. \quad (19)$$

The stiffness matrix of the interface has the form

77

$$\mathbf{K}_{int}(\omega_h) = \int_{\Gamma_{int}} \frac{G}{\Delta^2} \left( \frac{1}{\mathbf{N}_{\omega,h}(\mathbf{x}) \omega_h} - 1 \right) \mathbf{N}_{\llbracket u \rrbracket,h}^T(\mathbf{x}) \beta \mathbf{N}_{\llbracket u \rrbracket,h}(\mathbf{x}) d\Gamma \quad (20)$$

and the vector  $\mathbf{p}_h$  is expressed as

78

$$\mathbf{p}_h = \int_{\Gamma_{int}} G(\mathbf{x}) \mathbf{N}_{\omega,h}(\mathbf{x}) d\Gamma. \quad (21)$$

The minimization (12) is done by the alternate minimization approach which can be written as

79

80

$$(\mathbf{u}_k(\mathbf{x}), \llbracket \mathbf{u} \rrbracket_k(\mathbf{x}), \omega_k(\mathbf{x})) = \arg \min_{\omega(\mathbf{x})} \left( \min_{(\mathbf{u}(\mathbf{x}), \llbracket \mathbf{u} \rrbracket(\mathbf{x}))} \Pi_k(\mathbf{u}(\mathbf{x}), \llbracket \mathbf{u} \rrbracket(\mathbf{x}), \omega(\mathbf{x})) \right). \quad (22)$$

The minimization with respect to  $\mathbf{u}(\mathbf{x})$  and  $\llbracket \mathbf{u}(\mathbf{x}) \rrbracket$  is associated with the Lagrangian function in the form

81

82

$$\begin{aligned}
 L_{k,h}(\mathbf{u}_h, [\mathbf{u}]_h, \lambda_h) &= \frac{1}{2} \sum_{j=1}^n \mathbf{u}_h^{(j)T} \mathbf{K}^{(j)} \mathbf{u}_h^{(j)} - \sum_{j=1}^n \mathbf{u}_h^{(j)T} \mathbf{f}_h^{(j)} + \\
 &+ \frac{1}{2} [\mathbf{u}]_h^T \mathbf{K}_{int}(\omega_h) [\mathbf{u}]_h + \lambda_h^T (\mathbf{B}_h \mathbf{u}_h - [\mathbf{u}]_h).
 \end{aligned} \tag{23}$$

Note that the displacement jumps  $[\mathbf{u}]_h$  are subject to the non-penetration condition  $\mathbf{B}_h [\mathbf{u}]_h \geq \mathbf{0}$ . In the current implementation, these constraints are converted to equalities by adopting a simple active set strategy based on the values of the Lagrange multipliers  $\lambda_h$ . There are three stationary conditions

$$\frac{\partial L_{k,h}}{\partial \mathbf{u}_h^{(j)}} = \mathbf{K}^{(j)} \mathbf{u}_h^{(j)} - \mathbf{f}_h^{(j)} + \mathbf{B}_{u,h}^{(j)T} \lambda_h = \mathbf{0}, \tag{24}$$

$$\frac{\partial L_{k,h}}{\partial \lambda_h} = \sum_{j=1}^n \mathbf{B}_{u,h}^{(j)} \mathbf{u}_h^{(j)} - [\mathbf{u}]_h = \mathbf{0}, \tag{25}$$

$$\frac{\partial L_{k,h}}{\partial [\mathbf{u}]_h} = \mathbf{K}_{int}(\omega_h) [\mathbf{u}]_h - \lambda_h = \mathbf{0}. \tag{26}$$

Equation (24) is the equilibrium equation for the  $j$ -th subdomain, (25) expresses the interface conditions and (26) defines the relationship between the Lagrange multipliers and the displacement jumps on the interface.

### 3 FETI Method

This section summarizes the notation and the basic relationships of the FETI method which is a non-overlapping domain decomposition method. More details can be found in references [1, 4] or [5]. The vector of unknowns is denoted by  $\mathbf{u}$ , the vector of prescribed forces is denoted by  $\mathbf{f}$  and the stiffness matrix is denoted by  $\mathbf{K}$ . Interface conditions for perfect and imperfect interaction have the form

$$\mathbf{B}\mathbf{u} = \begin{pmatrix} \mathbf{B}_c \\ \mathbf{B}_s \end{pmatrix} \mathbf{u} = \begin{pmatrix} \mathbf{0} \\ \mathbf{s} \end{pmatrix} = \mathbf{c}, \tag{27}$$

where  $\mathbf{s}$  denotes the jump between subdomain displacements.

After space discretization, the functional of energy has the form

$$\Pi = \Pi(\mathbf{u}, \lambda) = \frac{1}{2} \mathbf{u}^T \mathbf{K} \mathbf{u} - \mathbf{u}^T \mathbf{f} + \lambda^T (\mathbf{B}\mathbf{u} - \mathbf{c}), \tag{28}$$

where  $\lambda$  denotes the vector of Lagrange multipliers.

The interface condition and the solvability condition define the coarse problem

$$\begin{pmatrix} \mathbf{F} & \mathbf{G} \\ \mathbf{G}^T & \mathbf{0} \end{pmatrix} \begin{pmatrix} \lambda \\ \alpha \end{pmatrix} = \begin{pmatrix} \mathbf{d} - \mathbf{c} \\ \mathbf{e} \end{pmatrix}, \tag{29}$$

where the well-known notation

$$\mathbf{F} = \mathbf{BK}^+\mathbf{B}^T, \quad \mathbf{G} = -\mathbf{BR}, \quad \mathbf{d} = \mathbf{BK}^+\mathbf{f}, \quad \mathbf{e} = -\mathbf{R}^T\mathbf{f} \quad (30)$$

is used.

In reference [6], a constitutive law for the Lagrange multipliers and the discontinuity was introduced in the form

$$\mathbf{c} = \mathbf{H}\boldsymbol{\lambda}, \quad (31)$$

where the compliance matrix,  $\mathbf{H}$ , was defined. The coarse problem can be rewritten to the form

$$\begin{pmatrix} \mathbf{F} + \mathbf{H} & \mathbf{G} \\ \mathbf{G}^T & \mathbf{0} \end{pmatrix} \begin{pmatrix} \boldsymbol{\lambda} \\ \boldsymbol{\alpha} \end{pmatrix} = \begin{pmatrix} \mathbf{d} \\ \mathbf{e} \end{pmatrix}. \quad (32)$$

The system of equations (32) is solved by the modified preconditioned conjugate gradient method.

Comparison of (26) and (31) reveals the following equalities

$$\mathbf{c} = [[\mathbf{u}]]_h = \mathbf{H}\boldsymbol{\lambda} = \mathbf{K}_{int}^{-1}(\omega_h)\boldsymbol{\lambda}_h. \quad (33)$$

## 4 Numerical Examples

The proposed strategy is applied to the end-notched flexure (ENF) test and the mixed-mode flexure (MMF) test used in reference [8]. The set up of the tests is depicted in Fig. 2. The material parameters are the following: Young's modulus of elasticity  $E =$

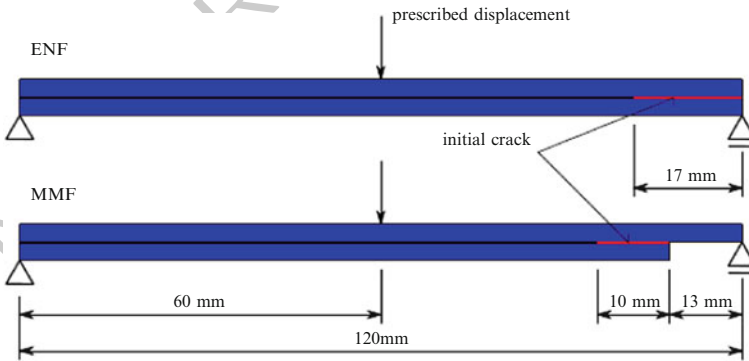


Fig. 2. End-notched flexure (ENF) and mixed-mode flexure (MMF) tests

75 GPa, Poisson's ratio  $\nu = 0.3$ , critical stress  $\sigma_{max} = 3.602$  MPa, critical opening  $\Delta = 0.011$  mm, fracture toughness  $G = 0.02$  N/mm, mode mixity parameter  $\beta = 0.472$ . The structures are discretized by quadrilateral finite elements with bi-linear basis functions. They are loaded by prescribed displacements in the center.

The load-deflection curves for both tests are depicted in Figs. 3 and 4. Very good agreement with results published in [8] and [7] is obtained.

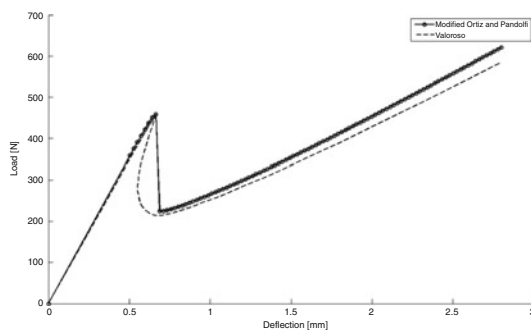


Fig. 3. Load-deflection curves for ENF test

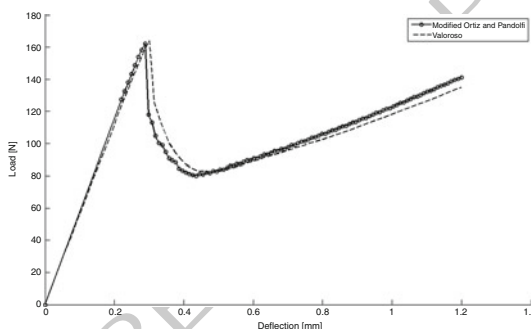


Fig. 4. Load-deflection curves for MMF test

## 5 Conclusions

119

Description of the imperfect material interface based on the compliance matrix  $\mathbf{H}$  introduced in [6] was generalized with help of the energy-based delamination model described in [2]. This formulation uses piecewise constant approximation of damage variables and as such it allows to express the interfacial stiffness matrix easily.

**Acknowledgments** Financial support for this work was provided by project number VZ 03 CEZ MSM 6840770003 of the Ministry of Education of the Czech Republic. The financial support is gratefully acknowledged.

## Bibliography

127

[1] Charbel Farhat and François-Xavier Roux. Implicit parallel processing in structural mechanics. *Comput. Mech. Adv.*, 2(1):124, 1994. ISSN 0927–7951.

- [2] Pavel Gruber and Jan Zeman. A rate-independent model for composite materials with imperfect interfaces based on energy minimization. In B. H. V. Topping, J. M. Adam, F. J. Pallarés, R. Bru, and M. L. Romero, editors, *Proceedings of the Seventh International Conference on Engineering Computational Technology*, Stirlingshire, Scotland, 2010. Civil-Comp Press. paper 10.
- [3] C.Y. Huia, A. Ruina, R. Long, and A. Jagota. Cohesive zone models and fracture. *The Journal of Adhesion*, 87:1–52, 2011.
- [4] Jaroslav Kruis. Domain decomposition methods on parallel computers. In B. H. V. Topping and C. A. Mota Soares, editors, *Progress in Engineering Computational Technology*, pages 299–322. Saxe-Coburg Publications, Stirling, Scotland, UK, 2004.
- [5] Jaroslav Kruis. *Computational Technology Reviews*, volume 3, chapter Domain Decomposition Methods in Engineering Computations. Saxe-Coburg Publications, Stirlingshire, Scotland, 2011.
- [6] Jaroslav Kruis and Zdeněk Bittnar. Reinforcement-matrix interaction modeled by FETI method. In *Domain decomposition methods in science and engineering XVII*, volume 60 of *Lect. Notes Comput. Sci. Eng.*, pages 567–573. Springer, Berlin, 2008. doi: 10.1007/978-3-540-75199-1\_71. URL [http://dx.doi.org/10.1007/978-3-540-75199-1\\_71](http://dx.doi.org/10.1007/978-3-540-75199-1_71).
- [7] M. Ortiz and A. Pandolfi. Finite-deformation irreversible cohesive elements for three-dimensional crack propagation analysis. *International Journal for Numerical Methods in Engineering*, 44:1267–1282, 1999.
- [8] N. Valoroso and L. Champaney. A damage-mechanics-based approach for modelling decohesion in adhesively bonded assemblies. *Engineering Fracture Mechanics*, 73:2774–2801, 2006.